New Mexico Geological Society

Downloaded from: https://nmgs.nmt.edu/publications/guidebooks/53

Third-day road log, from Alamogordo to White Sands, San Agustin Pass, Organ quarry, and Tortugas Mountain

Virgil W. Lueth, Spencer G. Lucas, Katherine A. Giles, Barry S. Kues, and James Witcher
2002, pp. 53-73. https://doi.org/10.56577/FFC-53.53

in:

Geology of White Sands, Lueth, Virgil; Giles, Katherine A.; Lucas, Spencer G.; Kues, Barry S.; Myers, Robert G.; Ulmer-Scholle, Dana; [eds.], New Mexico Geological Society 53rd Annual Fall Field Conference Guidebook, 362 p. https://doi.org/10.56577/FFC-53

This is one of many related papers that were included in the 2002 NMGS Fall Field Conference Guidebook.

Annual NMGS Fall Field Conference Guidebooks

Every fall since 1950, the New Mexico Geological Society (NMGS) has held an annual Fall Field Conference that explores some region of New Mexico (or surrounding states). Always well attended, these conferences provide a guidebook to participants. Besides detailed road logs, the guidebooks contain many well written, edited, and peer-reviewed geoscience papers. These books have set the national standard for geologic guidebooks and are an essential geologic reference for anyone working in or around New Mexico.

Free Downloads

NMGS has decided to make peer-reviewed papers from our Fall Field Conference guidebooks available for free download. This is in keeping with our mission of promoting interest, research, and cooperation regarding geology in New Mexico. However, guidebook sales represent a significant proportion of our operating budget. Therefore, only *research papers* are available for download. *Road logs*, *mini-papers*, and other selected content are available only in print for recent guidebooks.

Copyright Information

Publications of the New Mexico Geological Society, printed and electronic, are protected by the copyright laws of the United States. No material from the NMGS website, or printed and electronic publications, may be reprinted or redistributed without NMGS permission. Contact us for permission to reprint portions of any of our publications.

One printed copy of any materials from the NMGS website or our print and electronic publications may be made for individual use without our permission. Teachers and students may make unlimited copies for educational use. Any other use of these materials requires explicit permission.

This page is intentionally left blank to maintain order of facing pages.

THIRD-DAY ROAD LOG, FROM ALAMOGORDO TO WHITE SANDS, SAN AGUSTIN PASS, ORGAN QUARRY, AND TORTUGAS MOUNTAIN

VIRGIL W. LUETH, SPENCER G. LUCAS, KATHERINE A. GILES, BARRY S. KUES AND JAMES WITCHER

Assembly point: Holiday Inn Express in Alamogordo
Departure time: 8:00 AM
Distance: 83.9 mi.
Stops: 3

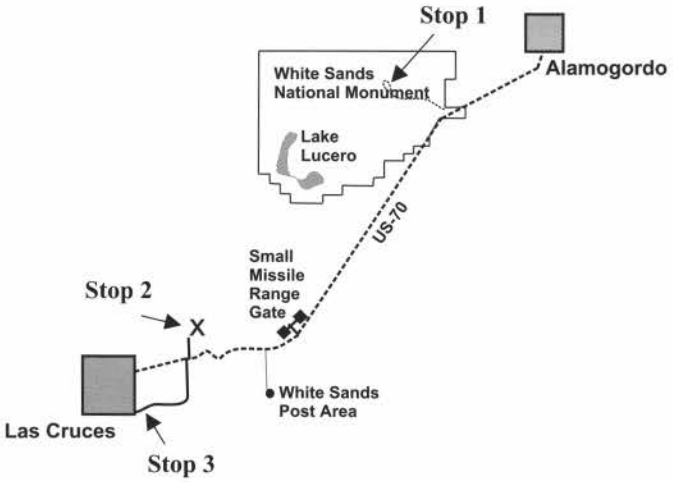

SUMMARY

Today's trip begins with a quick traverse of the southern part of the Tularosa basin with a stop at the world famous White Sands National Monument. We will then continue our traverse as we proceed up an out of the basin and onto San Agustin Pass, which separates the Organ and San Andres Mountains. We continue across the pass to enter the structural boundary zone between the Jornada del Muerto (to the north) and the Mesilla (to the south) basins of the Rio Grande rift. Here, we stop to examine the northern end of the Organ batholith, in the southernmost San Andres Mountains and the interactions between igneous intrusions and their host rocks that resulted in a variety of ore deposit types. The trip then proceeds south, along the spectacular western flank of the Organ Mountains. The route then traverses to the southwest into the Mesilla basin for the final stop at Tortugas ("A") Mountain. Here, we discuss paleo hot springs deposits and modern hydrology on the margins of a rift basin.

0.0/83.9 Parking lot at Holiday Inn Express in Alamogordo; leave lot, **turn left** on White Sands Blvd. (US 70 & 54). Proceed west toward Las Cruces. **(0.1)**

0.1/83.8 Traffic light at Panorama Blvd, **continue straight**. **(0.2)**

0.3/83.6 Cross bridge over railroad **(0.4)**

0.7/83.2 Junction with US-54 South; **continue straight**, west on US-70. Highway is resting on sand and gravel deposited by streams originating in the Sacramento Mountains. Here the sediments rest as a thin mantle on a flat pediment surface. We are beginning our traverse of the Tularosa basin, which covers an area of almost 17,000 km^2 in Sierra, Lincoln, Doña Ana and Otero Counties in southern New Mexico (King and Harder, 1985; Lozinsky and Bauer, 1991). Bordered to the west by the Oscura, San Andres, Organ and Franklin Mountains, and to the east by the Sierra Blanca and the Sacramento Mountains, the Tularosa basin is one of the few Rio Grande rift basins with internal drainage (Fig. 3.1). Structurally, it is two north-trending half grabens separated by the buried Jarilla fault zone (Fig. 3.2). In the western half graben, at least 6000 ft of Neogene sediments are basin fill and have been referred to the Santa Fe Group.

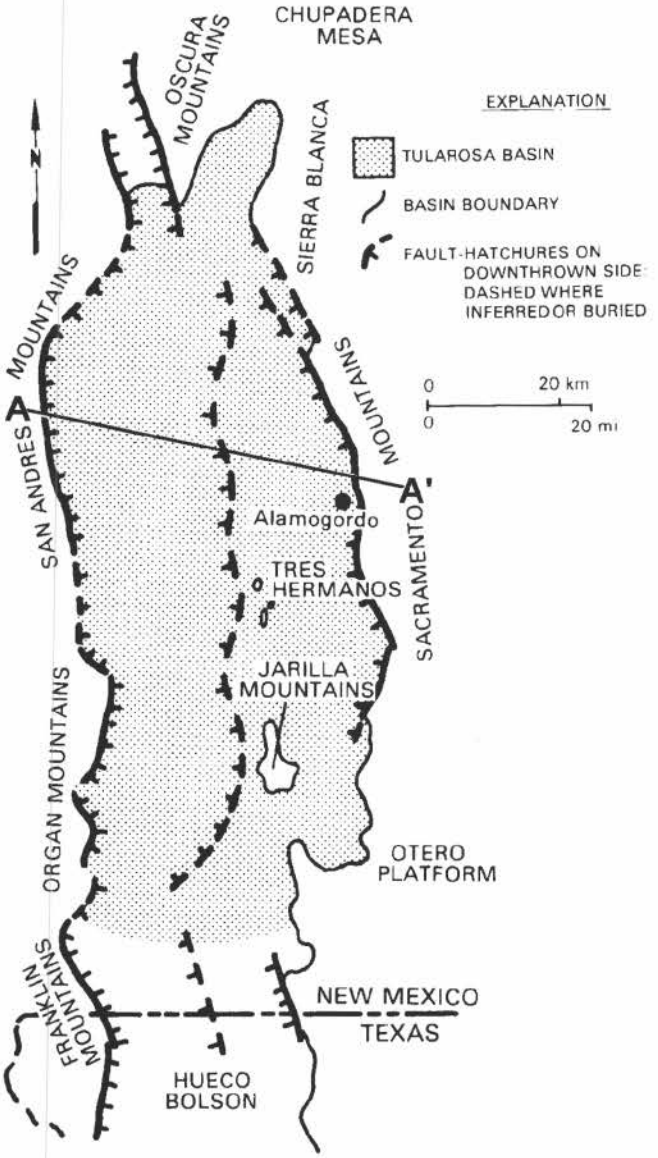

FIGURE 3.1. Map of the Tularosa basin (modified from Colpitts, et al., 1991)

Here, we are driving over a much thinner Neogene basin fill. The Jarilla fault zone, which is the structural boundary between the two half grabens of the Tularosa basin, is still 19 miles to the west of us. **(0.7)**

1.4/82.5 Light at Walker Avenue intersection; **continue straight. (1.1)**

2.5/81.4 Stop light at Airport Road, left; **continue straight**. Note Organ Mountains at 9:30 and the San Andres Mountains form the skyline from 10:00 – 3:00 on western side of the Tularosa basin. The Sacramento Mountains define the eastern side of the physiographic basin here. **(0.8)**

3.3/80.6 Cross under powerlines; Jarilla Mountains at 10:00; Tres Hermanos hills, in foreground at 10:30 (Fig. 3.3). The larger hills are mostly Permian Yeso Formation capped by limestone of the Permian San Andres Formation. The smaller, easternmost hills are composed of Permian Hueco Group limestone. The southernmost butte is a small stock of granodiorite similar to the early phase stock in the Jarilla Mountains (Eocene-Oligocene). The granodiorite is cut by a phase similar to the main phase monzonite-porphyry stock (Eocene-Oligocene) in the Jarilla Mountains. **(3.6)**

6.9/77.0 Exit to Holloman Air Force Base on right, pass under overpass. The base was originally founded as the Alamogordo Army Air Field in 1942. A post office was established under the name of Monista in 1944. The name of the base was later changed to Holloman Air Force Base in 1948. It

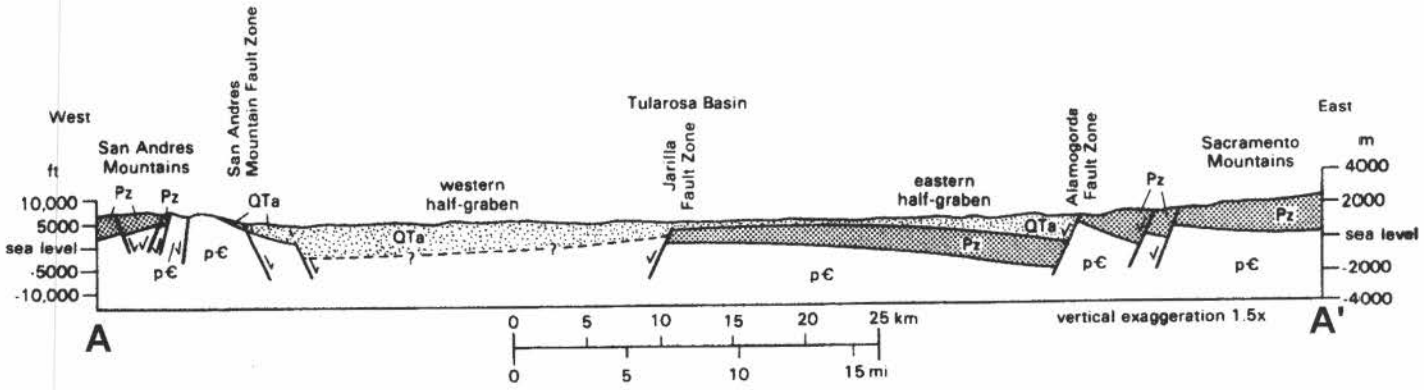

FIGURE 3.2. Cross section of Tularosa basin (modified from Colpitts, et al., 1991)

FIGURE 3.3. The Tres Hermanos.

is named to honor Col. George V. Holloman, a pioneer in guided missile research (Pearce, 1965) **(0.3)**

7.2/76.7 Note playa on left. **(0.9)**

8.1/75.8.8 Note gypsiferous sediments of Pleistocene Lake Otero on both sides of the road. **(0.5)**

8.6/75.3 Roadcuts on right well expose Pleistocene playa lake sediments. **(1.4)**

10.0/73.9 Playa lake bottom; Tres Hermanos at 9:00 – 10:00 on left. **(0.6)**

10.6/73.3 Mile Marker 203; outcrops on right are reworked eolian gypsum formed from Pleistocene lake sediments. This represents a microcosm of the process that formed the White Sands to be viewed later. **(0.1)**

10.7/73.2 Cross small playa lake (Fig. 3.4). The playa receives its water from the Holloman Air Force base water treatment plant. **(0.5)**

11.2/72.7 JOBE Concrete Products quarry on right. The quarry mined a small outcrop here of Permian age Hueco Group limestone for use in cement making. **(0.4)**

FIGURE 3.4. Playa near Holloman Air Force Base

11.6/72.3 Enter White Sands Missile Range. The fabled White Sands and this year's conference namesake can be seen ahead. **(1.0)**

12.6/71.3 Mile marker 201; North end of the Franklin Mountains can be seen in the distance at 10:30. Organ Mountains constitute the skyline at 11:00. The San Andres Mountains span the horizon from 12:00 to 2:00. **(1.4)**

14.0/54.9 **Turn right** into White Sands National Monument entrance on right (Fig 3.5). Employees quarters on left and visitor's center to right.

White Sands National Monument was established in 1933 and encompasses an area of 230 mi^2 (147,200 acres). The monument enables access to the most extensive and well studied gypsum dune field in North America via a 16-mile-long drive through the dunes. Herrick (1899) was one of the first geologists to write on the formation of the dunes, observing (p. 12) that "these great drifts are simply sand dunes collected from the gypsum sand formed as above stated on the surface of the lakes." (Fig. 3.6) **(0.2)**

14.2/69.7 Pass through entrance gate. We will be passing along the edge of the dunes for the next 2 miles. The text for the roadside exhibits is reproduced below. **(0.8)**

15.0/68.9 Exhibit on right.

"**Chihuahuan Desert**: North America's Largest and Highest Desert – The land before you is part of the distinctive Chihuahuan Desert, which extends into three American states and nine Mexican states. In New Mexico, this desert is characterized by strong winds, poorly-developed soils, scorching summer days, and freezing winter nights. Still, more than 240 species of plants and numerous animals thrive in this area. In this land of little rain, virtually all life has evolved ways to conserve water." **(0.8)**

15.8/68.1 Exhibit on right.

"**The Tularosa Basin**: Land of the Snowwhite Sands – Here, at the northern end

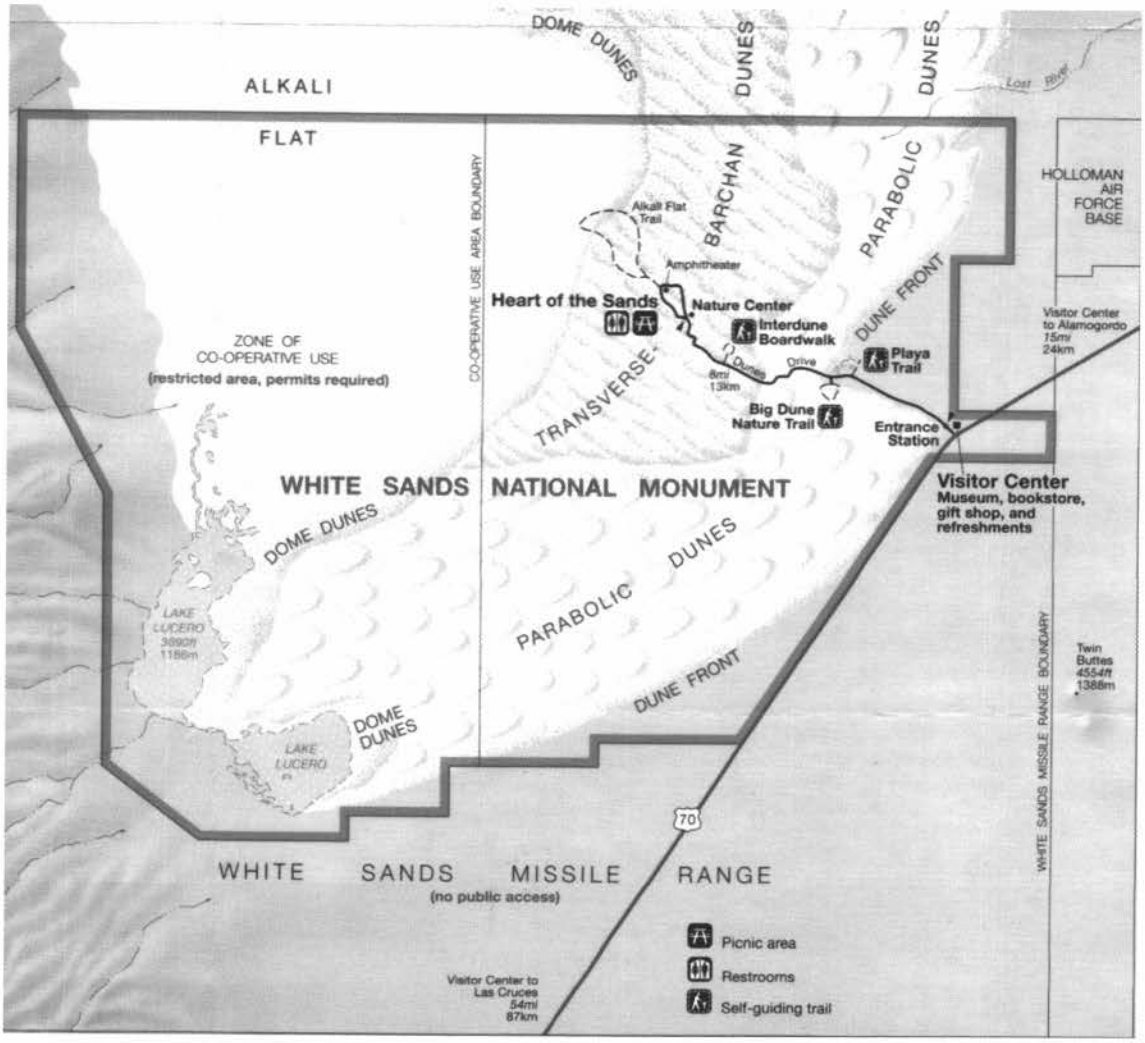

FIGURE 3.5. Map of White Sands National Monument (courtesy National Park Service).

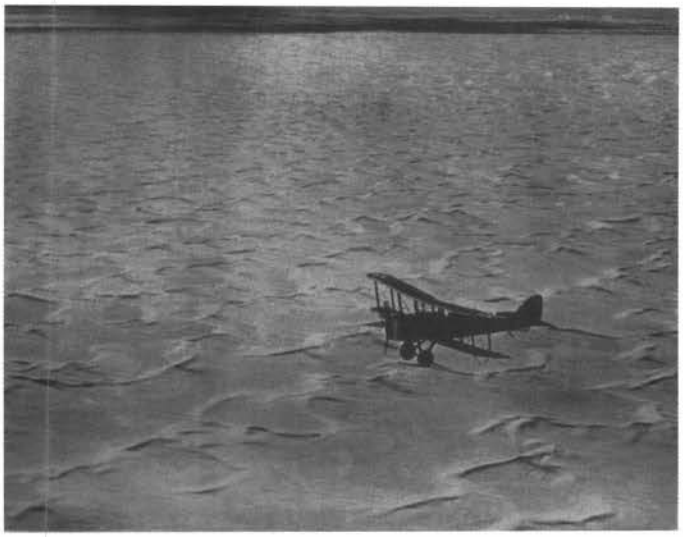

FIGURE 3.6. Biplane over the White Sands (Darton, 1928).

of the Chihuahuan Desert, in the center of the Tularosa Basin, lies the world's largest gypsum dune field. The gypsum that forms these dunes comes from the light-colored layers of rocks you see in the San Andres Mountains to your left and the Sacramento Mountains to your right. Rain and snow in these mountains dissolve the gypsum and carry it into the Tularosa Basin." **(0.8)**

16.6/67.3 Exhibit on right.

"**Playa:** A dry lake bed – Because no rivers drain the Tularosa Basin, gypsum-laden water from the surrounding mountains cannot escape to the sea. Instead, water collects in low areas and creates shallow, temporary lakes or playas, like the one in front of you. As the lakes

evaporate, the gypsum is left behind. Lake Lucero, a large playa at the base of the San Andres Mountains, behind you, is today the major source of gypsum sand for the dune field. Follow the 100 yard (90 meter) trail to explore this small playa." **(0.2)**

16.8/67.1 Big Dune Trailhead to left. Enter the sand dunes. **(0.1)**

16.9/67.0 Exhibit on right.

"**From Water to Wind**: The Creation of the Dunes – Without wind there would be no dunes. But once water has deposited gypsum in the playas, strong southwest winds, especially in the spring, blow across the dry surfaces of playas and move sand-size particles toward the northeast. Over the past several thousand years, the wind driven gypsum dunes around you have engulfed 275 square miles (712 km^2) of the Tularosa Basin." **(1.0)**

17.9/66.0 Exhibit on right

"**Slipping Ahead**: How sand dunes move – Sand is usually too heavy for the wind to move more than a few inches in the air. As a result, the gypsum sand grains roll or bounce along the ground and pile up into a dune. Sand builds up on the windward crest of a dune, until gravity pulls it down the leading edge, the slip face, in a miniature avalanche. In this way a dune moves forward a fraction of an inch at a time." **(0.5)**

18.4/65.5 Trailhead for interdune boardwalk and exhibit on right.

"**A Desert within a Desert**: Survival in the Shifting Dunes – Life is difficult in the dune field, even for plants of the Chihuahuan Desert. The conditions are unusually harsh: burial by moving dunes, nutrient-poor gypsum soils, and extreme fluctuations of temperature. Only about 60 species of plants, one quarter of those growing in the adjacent Tularosa Basin, have found a way to survive in the dunes." **(0.4)**

18.8/65.1 Exhibit on right.

"**Animal Life** – Animals are rarely seen within the dune field. The extreme temperature and lack of food, shelter and standing water combine to restrict their number. But they are here, even in the heart of the dunes.

Like plants, most animals are found in the interdunal flats. During the day look for beetles, lizards, and birds venturing out onto the sand." **(0.2)**

19.0/64.9 Sunset stroll trailhead on left. **(0.6)**

19.6/64.3 Pullout on left. **(0.4)**

20.0/63.9 Exhibit on right

"**Tracks in the Sand** – In order to conserve water and avoid extreme temperatures, many desert animals stay underground during the day. They emerge from their burrows only after sunset. Evidence of their activities can be found in the sand the next morning.

Even at night, dark animals are easily spotted against the white background of the gypsum sand, making them easy victims for predators. Some small animals, including pocket mice, lizards, and insects have evolved a light coloration that camouflages them in the dunes". **(0.2)**

20.2/63.7 Intersection with dune loop road. **(0.1)**

20.3/63.6 **STOP 1.** "Heart of the Dunes" Nature Center

Modern understanding of the gypsum dunes began with McKee's (1966) classic paper that documented in detail the eolian origin, growth and movement of the dunes (also see McKee and Douglass, 1971; McKee et al., 1971, and a summary by LeMone, l987) (Fig. 3.7). As McKee indicated, the gypsum source of the White Sands must ultimately be upper Paleozoic strata (Pennsylvanian Panther Seep Formation, Permian Yeso and San Andres formations, with the Yeso the probable major source) in the nearby mountain ranges (mainly the San Andres range), but the proximal source is mostly groundwater-leached evaporite deposits of Pleistocene Lake Otero. The origin of the gypsum sands began with leaching of gypsum from upper Paleozoic strata of the San Andres Mountains in the moister climate of the late Pleistocene, and

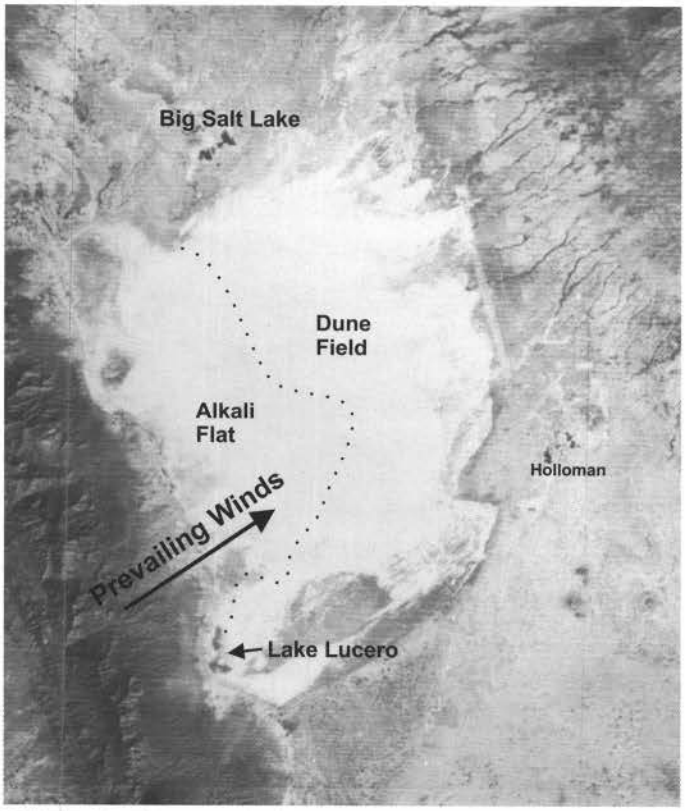

FIGURE 3.7. Diagrammatic illustration of a model for the formation of the White Sands. Gypsum from the Lake Lucero and Alkali Flat areas is blown by prevailing winds into a dune field.

runoff of the gypsum-bearing water into Lake Otero. As Lake Otero shrank in size at the end of the Pleistocene and through the Holocene, to become modern Lake Lucero, large amounts of gypsum were precipitated as selenite crystals (some up to 4 ft long) from the evaporating lake water, both on and within the sediments of the lake bed. Most of the selenite probably formed on mudflats during a late stage of Lake Otero, between the coarse-grained alluvium at the base of the San Andres range, and the fine-grained saline lacustrine deposits to the east. The dune grains are largely fragments spalled from these crystals by mechanical weathering and transported northeastward from the Lake Lucero area by the prevailing southwest winds. A wind velocity of 17 mph is necessary to move the grains, and Spring (especially March and April) sandstorms gusting up to 55 mph are a major factor in moving large volumes of gypsum sand. During wind activity, the clay and silt-sized particles are carried off in suspension while the larger grains are saltated to the dune field. The white color of the grains is the result of microfractures occurring as the grains are weathered and transported.

Allmendinger (1971) noted that during times of playa flooding by surface water, a crust may form, which thickens upon evaporation of the water, due to precipitation of gypsum from water rising through the sediment by capillary action. The crust becomes puffy and breaks down into a fine powder that is carried off in suspension in white clouds that may rise thousands of feet above the playa floor. Displacive action of crystallization also may bring up clear gypsum crystals 10 to 20 mm in diameter, which are subsequently broken down and moved by saltation to the dune fields. Deflation of grains from the original selenite deposits, together with grains derived from modern evaporite leaching groundwater brines, provide the sources for the gypsum sands. Surface waters are contributing little dissolved material to Lake Lucero.

The gypsum dune sand is mainly medium grained, tabular in shape, ranges from angular to subrounded, and is moderately to well sorted. Dunes up to 65 ft high develop by primary deposition resulting from settling from suspension, saltation, and creep, then redeposition by avalanching of the crest, and contemporaneous erosion (LeMone, 1987). In areas of active dune formation, the interdune flats may occupy the majority of the area. According to McKee and Douglass (1971), embryonic, dome-shaped dunes under constant, unobstructed wind conditions rarely exceed 18 ft in height and move 24 to 38 ft per year. Other dune types, and those that are anchored to some degree by vegetation, move less.

Four basic dune types are present within the White Sands dune field. Dome dunes extend from Lake Lucero in a thin band along the northwestern margin of the

field. Parabolic dunes (crescent-shaped dunes that are convex downwind, with arms anchored by vegetation) occupy much of the southern and eastern sides of the field. Barchan dunes (crescent-shaped and convex upwind, that form in strong winds but relatively little sand supply) occupy much of the northwestern area, farthest from the source of the grains. Transverse dunes (parallel ridges of sand formed by coalescence of barchan dunes) are present in the west-central part of the field, around the "Heart of the Sands" area at the end of the road leading northwest from the Monument visitor's center.

Detailed studies of internal dune morphology and bedding structures (see authors cited above) indicate that degree of sand moisture, algal laminae, fluctuations in sand supply and wind energy, and the mechanics of dune migration are all significant in shaping the dunes. The maximum age of the gypsum dune field at White Sands is l2,000 to 24,000 years.

After stop, proceed straight (north) on the dunes loop road. **(0.6)**

20.9/63.0 Gate and road to right to "Hollywood in the Dunes." This area is often used to "shoot" films and commercials using the white sands as a backdrop. **(0.3)**

21.2/62.7 Parking area for evening programs and rest facility. **(0.1)**

21.3/62.6 Exhibit on right.

"Heart of the Dunes – Do you see any plants growing on top of the dunes? In the center of the dune field, dune movement may exceed 10 feet (3 meters) per year. Here, even the most rapidly growing plants are buried. Only a few grasses and wildflowers able to grow between the dunes, until they are quickly overwhelmed." **(0.3)**

21.6/62.3 Alkali Flat trailhead to the right. **(0.6)**

22.0/61.9 Parking area to right. **(0.2)**

22.2/61.7 Picnic area. **(0.3)**

22.5/61.4 Back country camping area to right. **(0.1)**

22.6/61.3 Intersection with loop road, **turn right** and return to entrance. **(1.7)**

24.3/59.6 Note line of cottonwood trees on both sides of road. Actually, you are only viewing the upper branches of the trees since the are mostly buried by gypsum sand. Cottonwoods usually occur along faults in the monument. **(1.0)**

25.3/58.6 Notice the raised dark pillars to the right. These pillars mark paleo-campfires that cooked the gypsum, dehydrating it to anhydrite. Later rain reacted and created a "plaster" cap protecting the camping site from wind erosion. **(3.5)**

28.8/55.1 Pass entry gate, proceed straight. **(0.2)**

29.0/54.9 Intersection with US-70, **turn right. (0.1)**

29.1/54.8 U.S. Border Patrol – Immigration and Naturalization Service check point on left. **(2.4)**

31.5/52.4 "Point of Sands" at crest of the hill is dunes of white gypsum sand, at mile marker 197. Note Sacramento Mountains escarpment behind us; at 9:00 note Tres Hermanos hills. **(3.9)**

35.4/48.5 Crest of hill, again on the crest of a gypsum dune. In this vicinity, the Jarilla fault zone that defines the structural boundary between the two half grabens of the Tularosa Basin passes under the highway. We have crossed from a mantle of shallow basin fill onto a deeper structural basin with an estimated 6000 feet (1300 meters) of fill.

The Jarilla Mountains at 9:30 (Fig. 3.8) are a structural dome of upper Paleozoic (mostly Lower Permian Hueco Group:

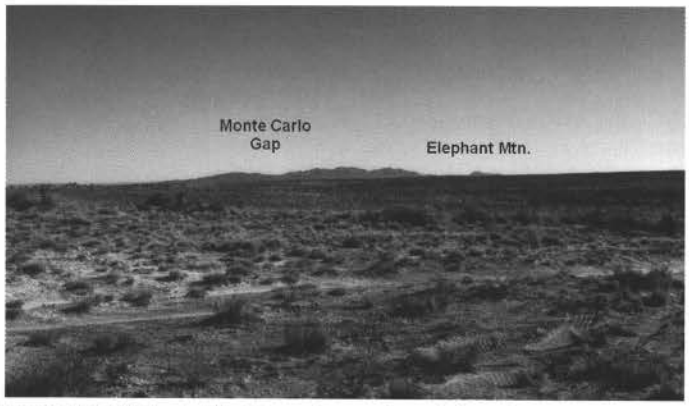

FIGURE 3.8. The Jarilla Mountains as viewed from the north.

see Lucas and Krainer, this volume) limestones intruded by Cenozoic igneous stocks, dikes and sills (Schmidt and Craddock, 1964). Mining of copper, lead, silver and gold lode ores and placer gold took place there between 1900 and 1930. A significant amount of iron mining was also done from skarn deposits in the district. The area remains a favorite of mineral collectors seeking turquoise veins and nodules, garnet, and magnetite crystals. **(1.2)**

GEOARCHEOLOGY OF THE JARILLA MOUNTAIN FANS AND ADJACENT TULAROSA BASIN FLOOR

William H. Doleman
Office of Contract Archeology, University of New Mexico, Albuquerque, NM 87131; wdoleman@unm.edu

INTRODUCTION

From 1985 to 1987, the UNM Office of Contract Archeology (OCA) conducted a series of cultural resource management projects on White Sands Missile Range in the southern Tularosa Basin. The study area comprised 225 sq. km on the west side of the Jarilla Mountains northwest of Orogrande, NM. The Border Star 85 project, funded by the US Army, was a systematic sample survey of the entire study area, followed by intensive survey of selected areas for the purposes of sample evaluation (Seaman et al. 1988). The Ground Based Laser project was funded by the Strategic Defense Command and entailed a more comprehensive survey of 20 sq. km within the original sample area, as well as excavation of portions of 33 archeological sites. Excavations yielded prehistoric cultural remains from both the Archaic (ca. 8000 B.C.-A.D. 400) and Formative (ca. A.D. 400-1400) periods, and thus covering the gradual transition from highly mobile hunting and gathering to incipient, and eventually full-reliance agriculture (Doleman et al. 1991, 1992). The undertaking of two large archeological projects in the same area offered a rare opportunity to identify, refine, and address research questions through staged fieldwork and analysis (Doleman 1995, 1997a).

In addition to typical questions of prehistoric adaptations, settlement, and chronology, OCA's research was guided by a recognition that surface-visible archeological remains in the project area are not amenable to the conventionally-drawn distinction between (a) archeological "sites" (clusters of artifacts and/or features interpreted as one or more "occupations"), and (b) "isolated occurrences" ("IOs", individual artifacts or limited clusters of similar artifacts interpreted as debris produced by off-site activities).

Archeological "sites" are an important construct not only for the study of prehistoric lifeways, but in cultural resource management because they are the primary unit of compliance with federal and state regulations. To be afforded some form of protection under federal law, archeological remains must qualify as a "site" and be determined to contain scientifically valuable information (datable materials, subsistence remains, structures, artifact assemblages, etc.). OCA's research built on previous researcher's questioning of the validity of the site concept (Ebert 1986; Foley 1981; Rossignol and Wandsnider 1992).

During the Border Star 85 survey, field archeologists were commonly frustrated in their attempts to define archeological sites. This problem was due in part to the obscuring effects of local eolian coppice dune deposits and intervening blowouts, and in part to the semi-continuous nature of the underlying distribution of archeological features and artifacts. In many broad areas, almost every blowout contained at least a few artifacts, and discrete site boundaries were impossible to define.

Recognition of this problem suggested two important conclusions. First, significant methodological biases result from applying conventional survey techniques to non-discrete surface distributions, including the fact that lower discovery rates for low-density surface remains offers false confirmation of the site/IO distinction. Secondly, surface remains have been subjected a number of geomorphic biases that affect their content and perceived distribution. Succeeding project phases were designed to evaluate these hypotheses with the eventual goal of analyzing survey-documented project area surface distributions in terms of changing land use patterns across the Archaic-Formative transition.

Crucial information for evaluating these conclusions was derived from two sources. The first was a geomorphic study including excavation of 104 trenches and documentation of 70 stratigraphic profiles on the western Jarilla Mountain, bajada and basin floor (Blair et al. 1990a, 1990b). This study provided important information on the geomorphic context of archeological remains, as well as an understanding of the relationship between the distribution of those remains and the paleolandscape. The second was excavation of portions of archeological sites in a variety of geomorphic settings. Data recovered yielded 34 radiocarbon dates as well as evidence of geomorphic effects on both surface and subsurface remains.

The Jarilla Mountains are a Tertiary igneous stock that measures ca. 5 by 13 km north-south and whose highest point stands some 435 m above the 1330 m elevation of the surrounding basin floor. The following discussion draws heavily on the geomorphic study of Blair et al. (1990a, 1990b). Two geomorphic zones were identified in the study area representing separate but interacting depositional environments. The first is the gently sloping bajada, which lies at the foot of the mountain front and grades into the second zone, the nearly flat basin floor. Surficial deposits of the basin floor consist of an eolian sand-sheet underlain by Pleistocene-age lacustrine, alluvial, and eolian sediments deposited along the margin of Pleistocene Lake Otero over older Camp Rice Formation sediments. Although the overall morphology of the bajada is controlled by Pleistocene alluvial fan deposits, the upper portions contain greater than 50 percent eolian sediments and consist of a sand ramp capped with a thin desert pavement. The basin floor and bajada topographies and geomorphic pro-

cesses blend and interact in a transition zone where bajada-draining channels and arroyos feed ephemeral channel-mouth ponds that are coincident with deflation depressions at the interface between the bajada and basin floor environments.

Since the late Pleistocene recession of Lake Otero, eolian processes have dominated the area's geomorphic history throughout terminal Pleistocene and Holocene times. Four Quaternary stratigraphic units, ranging in estimated age from 100 to ca. 130,000 years BP, were identified in the trench network. These units document cycles of erosion, deposition, landscape stability, and soil formation in the study area, with the lower three units exhibiting buried soils (locally-exhumed) capped by regionally recognized bounding surfaces.

Unit Q1 (the oldest) comprises late Pleistocene lacustrine and eolian deposits, as well as true alluvial fan deposits in the bajada. The unit has generally been stripped to a K horizon with stage III (to IV locally) carbonate morphology, although a Btk horizon is locally preserved above the K horizon in the upper bajada. Subsequent depositional units are entirely eolian in origin.

Unit Q2 overlies Q1, has been extensively stripped, and commonly exhibits a moderately-developed Btk horizon with stage II carbonate morphology, moderate structure, and abundant pedogenic clay. Locally, the Btk is underlain by a Bk.

Unit Q3 contains the study area's youngest buried soil and exhibits a locally preserved A/Bw sequence underlain by a Bk horizon with stage I carbonate development. Unit Q3 contains most of the archeological remains of the project area. Radiocarbon ages derived from Unit Q3 cultural contexts range from 4075-440 yr. BP (cal. 2584 B.C.-A.D. 1446). The humate fraction of a bulk sample of the Q3 A horizon yielded a radiocarbon age of 160 +/- 90 yr. BP (cal. A.D. 1679-1947), an age that likely underestimates the soil's true age (Wang and Amundson 1996). The Q3A horizon, which generally exhibits flat to gently sloping topography, probably represents a landscape characterized by stabilizing grassland vegetation.

Unit Q4 consists of recent eolian deposits lacking any evidence of soil formation. The unit represents an erosional cycle that began no more than about 150 years ago with the breakup of the stable Unit Q3 desert grassland. The most common forms of Q4 deposits are mesquite-capped coppice dunes and reworked surface deposits on blowouts.

Based on similarities in soil development as well as radiocarbon dates from Q3 contexts, units Q1-Q3 have been correlated with the Jornada II, Isaacks' Ranch, and Organ units of the Desert Project (Gile et al. 1981), and are thus estimated to date as follows. Q1: 130,000 to >15,000 yr., Q2: 15,000-9,000 yr., and Q3: 7300-150 yr.

Analyses of archeological data were focused at two scales: (a) surveyed site distributions, and (b) intra-site distributions of excavated remains. The following summarizes information presented in Anschuetz et al. (1990), Doleman et al., (1992), and Doleman (1995, 1997a, 1997b).

Three scales of important topographic variation are present in the study area. These are, from largest to smallest, (a) major landforms such as the bajada and basin floor and (1s-10s of km); (b) the various eolian landforms such as mounds and swales (10s-100s of m; termed "macrotopography" here), and (c) the microtopography of local surface eolian features such as coppice dunes (1s to 10s of m). Blair et al. (1990a, 1990b) concluded that the present macotopography is the same as that of the mid-to-late Holocene, although my analysis of trench data indicates that elevational differences between intermediate-scale landforms are greater than average Q2 and Q3 unit thickness variations by an order of magnitude, suggesting the macrotopography is at least as old as the early Holocene erosion of Q2 (Doleman 1995). The fact that the modern and prehistoric topographies are essentially identical is important, because existing macrotopographic variations are indicators of the prehistoric landscape characteristics.

At the larger scale of analysis, photo-interpretation of stereopairs of 1:18,000-scale air-photos of the project area was used to prepare a GIS map of the macrotopography, with high and low areas variously identified as sand mounds, depressions, and other eolian and bajada landforms. Comparison of the distribution of surveyed site locations with the mapped macrotopography yielded statistically significant correlations between sites and almost all of the "high" landforms, including bajada, transition, and basin floor geomorphic zones (Fig. 3.9). Moreover, recovery of archeological materials from deep, inter-blowout deposits yielded two important conclusions. First, on macrotopographic highs, archeological remains are more continuously distributed than surface manifestations imply. This in turn implies that the "real" sites are the highs themselves. Second, the Q4 deposits' alternating coppice dune/blowout topography significantly affects the surface visibility of extant archeological remains. Despite significant differences in average Q4 thickness across the project area, however, the blowouts tend to ensure detection of at least some archeological materials.

At the scale of the individual site, analyses focused on evaluating the relative contributions of prehistoric behavior and geomorphic processes to the spatial structure of both the surface and combined surface/subsurface archeological records. The presence at some sites of feature-associated artifact distributions indicated that behaviorally-conditioned small-scale spatial patterning in artifact distributions was present and had not been completely obliterated by geomorphic processes.

Analyses of data from excavated sites also provided insights into the effects of geomorphic and biological processes on surface and subsurface archeological assemblages. Analyses confirmed the expectation (Wandsnider 1989) that vertical size sorting of artifacts occurs in eolian surface deposits, but also confirmed vertical size-sorting within intact Stratum Q3 deposits. The latter might result from bioturbation, or the cumulative effects of repeated blowout formation and infilling. In both cases, smaller and flatter artifacts tend to be buried in surface contexts and to lie deeper in buried deposits. Finally, analysis comparing artifact distributions from blowouts in varying stages of formation concluded that blowout formation processes appear to affect horizontal artifact distributions by initially increasing density and assemblage aggregation through concentration (a phenomenon termed the "funnel effect"). Subsequently, however, the patterns produced by this effect are replaced by randomization resulting from blowout expansion and merging.

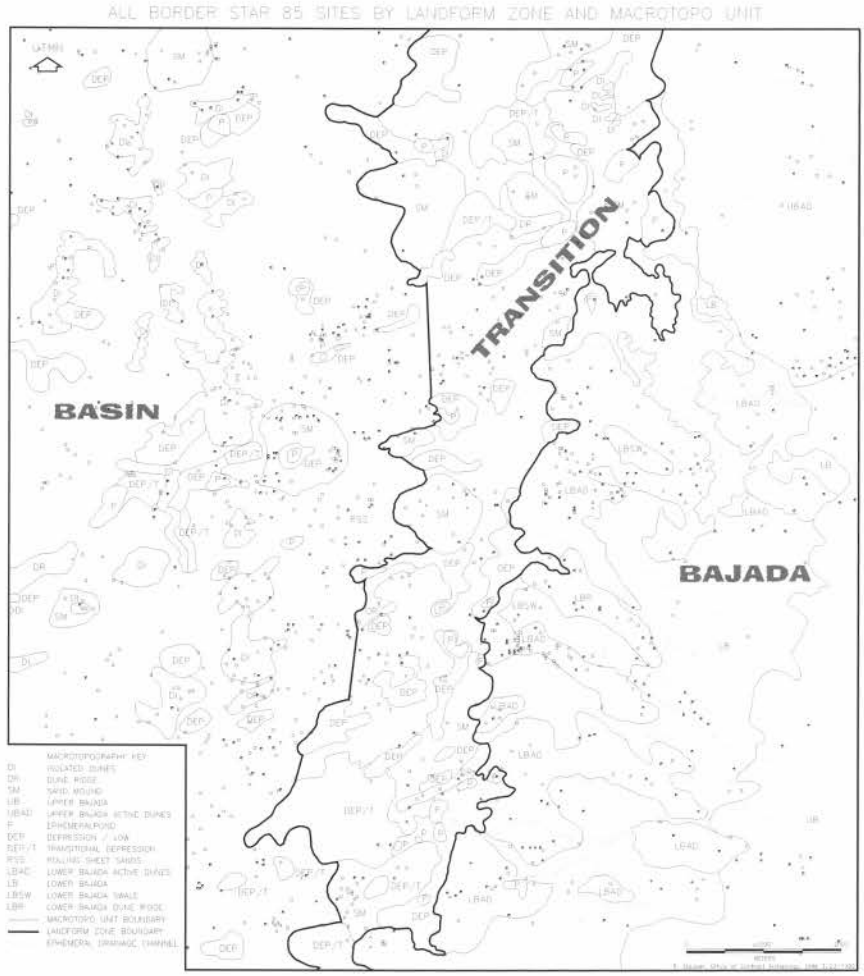

FIGURE 3.9. Distribution of Border Star 85 survey archeological sites with respect to geomorphic zones and macrotopography (straight zone boundary lines indicate areas where boundary could not be easily defined).

36.6/47.3 Milepost 192 and small rest area on right. **(2.0)**

38.6/45.3 Milepost 190 at dune crest, Organ Mountains dead ahead. **(2.9)**

41.5/42.4 Road passes through non-gypsum dunefield. **(1.0)**

42.5/41.4 Buildings at right at Route 264 intersection. Ahead is an excellent view of the east face of the Organ Mountains (Fig. 3.10). Sugarloaf Peak is a large granite exfoliation dome consisting of Sugarloaf Peak quartz monzonite (Seager, 1980) in the center of the range from this perspective. Organ Needles north of Sugarloaf consist of quartz syenite and quartz-alkali feldspar syenite and represent an early phase of the Organ batholith that predates the Sugarloaf Peak rocks. **(1.1)**

43.6/40.3 Milepost 185; Bear Canyon in the San Andres Range at 2:00. **(3.0)**

46.6/37.3 Milepost 182; Large alluvial fan at the base of Rocks Springs Canyon at 12:30. Monte Carlo Gap in the Jarilla Mountains at 8:30. Hueco Mountains at 9:30; Frank-

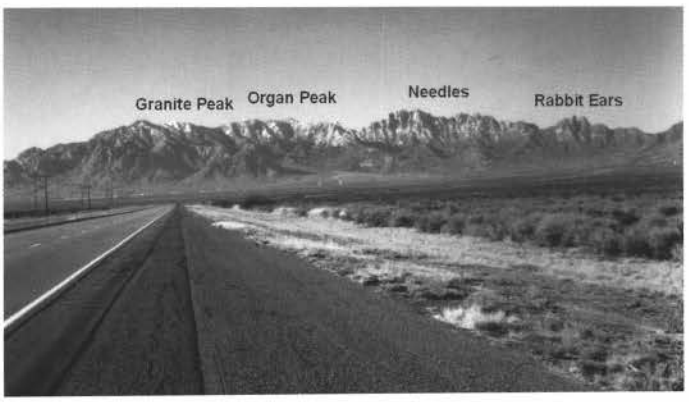

FIGURE 3.10. East face of the Organ Mountains

lin Mountains at 11:00; Antelope Hill at 12:00; Mineral Hill at 1:00. **(3.0)**

49.6/34.3 Road cut through non-gypsum dune form with slip face to west. **(1.0)**

50.6/33.3 Road crests hill (dunes). Historical Marker on left at milepost 178 for Albert J. Fountain. Albert Jennings Fountain was a Civil War veteran, New Mexico legislator and prominent lawyer. Colonel Fountain and his young son were presumed murdered near this spot while traveling between Lincoln and Las Cruces on February 1, 1896. Their bodies have never been found. Oliver Lee and James Gilliland were tried for their murder in 1898. Both were acquitted. A good view of the northern Franklin Mountains can be seen at 10:00. **(0.2)**

50.8/33.1 Leaving Otero County, entering Doña Ana County. **(3.4)**

54.2/29.7 Entrance to the Small Missile Range (SMR) on right. This is the endpoint of yesterday's second-day roadlog. **(2.4)**

56.6/27.3 Mile marker 172. Note east dipping Paleozoic rocks to the right on the eastern flank of the southern San Andres Mountains. These are mostly much deformed Cambro-Ordovician strata of the Bliss Formation and El Paso Group (Seager et al., 1987). San Agustin Peak, the pointed peak north of San Agustin Pass, is composed of Sugarloaf Peak quartz monzonite. It takes on the pointed shape because of two felsic dikes that pass near the top, creating a wedge of granite between the more easily eroded dikes. **(2.0)**

58.6/25.3 Missile Range HQ exit on right. The road to HQ is called Owen Road, named after Pfc. Marvin R. Owen. A memorial posted at the site of the tragedy where Pfc. Owen died reads:

"On 19 August 1978, Pfc. Marvin R. Owen, A Military Policeman assigned to the 259th Military Police Company, without thought for personal safety, drove his military police vehicle onto Las Cruces Access Road Bridge, already covered with flood waters, to assist a vehicle in immediate danger of being washed away. Pfc. Owen parked his vehicle as a shield to the endangered vehicle in a valiant attempt to prevent death to the family of four that was trapped inside. Ultimately both vehicles were swept from the bridge by a wall of water estimated to have been 10 to 12 feet high, taking with it Pfc. Owen's as well as the family of four live,"

That same flood washed out the access road to Aquirre Springs Recreation area farther up the mountain.**(1.0)**

59.6/24.3 Proterozoic granite and granite gneiss on both sides of the road. Hill on the left is Antelope Hill, consisting of Proterozoic granite projecting through a thin mantle of Plio-Pleistocene Camp Rice Formation. To the right is Mineral Hill, the site of numerous small mines. The hill is composed of Proterozoic granite cut by altered diabase (epidiorite of Dunham, 1935) and presumably Tertiary age rhyolite dikes. Ore mineralization is typically found in veins on the margins of these diabase dikes (Fig. 3.11). One group of mines is centered around Mineral Hill, and a second group is located about two miles north-northeast. Geologic descriptions and assay data for the deposits can be found in Dunham (1935), and a more recent evaluation is McLemore et al. (1996). **(1.2)**

60.8/23.1 Granite Peak to left. Organ Mountains fault of Seager (1980) displacing modern sediments on the Rock Springs Canyon alluvial

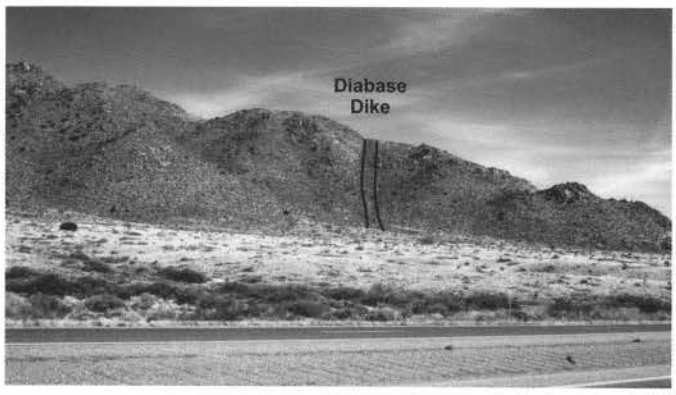

FIGURE 3.11. The Lady Hopkins mine on Mineral Hill. Mineralization is located at the granite – diabase contact.

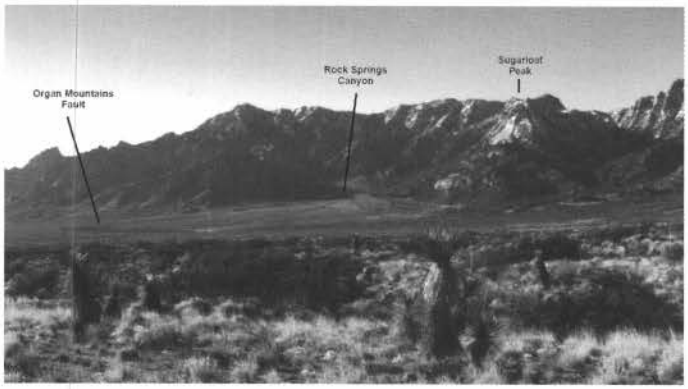

FIGURE 3.12. Organ Mountains Fault west of White Sands Missile Range Headquarters.

fan at 9:00 (Fig. 3.12). This late Holocene displacement was the subject of a study by L. H. Gile (1987). Alluvial fan deposits, of several different ages, have been displaced several times in the same place. Soil morphology, geomorphic and stratigraphic evidence indicates that major displacement took place at 1,000 B.P., and maximum displacement is estimated at 14 feet. **(2.3)**

63.1/20.8 Leaving White Sands Missile Range. Black Prince Canyon at 3:00 (Fig. 3.13). Proterozoic rocks are in fault contact with lower Paleozoic rocks at the head of the canyon. The fault is mapped as an east-dipping, high angle reverse fault called the Black Prince fault by Seager (1980).

The Black Prince mine consists of irregular replacement deposits of galena hosted in Silurian Fusselman Dolomite located at the base of the Devonian Percha Shale. The deposits are located at the base of the canyon about a mile north of the highway. Higher up on the west side of the canyon is the Hilltop Mine. The Hilltop is a similar type of deposit, but rich in tellurium. In addition to the replacement deposits that consist of galena, sphalerite and pyrite, a small silicified zone is found at the base of the replacement ore that contained significant gold values. Lueth (1998) suggests the silicified ores represent a second episode of mineralization that was high in gold and tellurium and overprinted the sulfur-rich base metal ores. From time to time, the Hilltop Mine has been mined for specimens of the mineral Altaite (lead telluride). Some specimens were sold to Wards Scientific Company and later distributed to mineralogy classes around the world. **(0.3)**

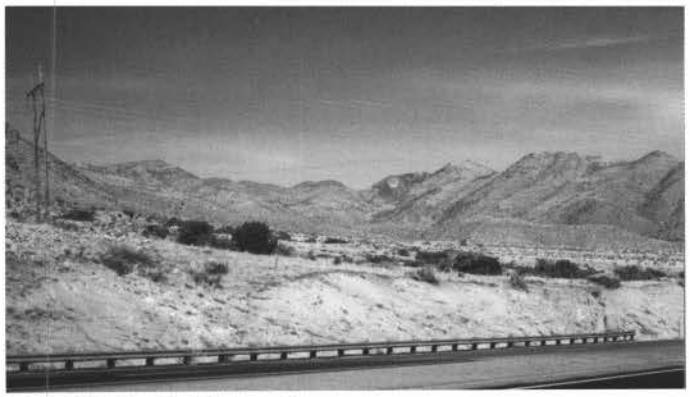

FIGURE 3.13. Black Prince Canyon

63.4/20.5 Road to Aguirre Springs Recreation Area on left. Galloway flow banded rhyolite dike in roadcut to right. **(0.2)**

63.6 /20.3 Excelsior dike in roadcut to right, a flow banded rhyolite identical to the Galloway dike. Both the Excelsior and Galloway dikes can be traced over 4 miles across the crest of the range. Stop 2 will visit these dikes at their western extent. A number of ore deposits are associated with this dike trend (Fig. 3.14). **(0.6)**

64.2/19.7 Missile on left as we approach San Agustin Pass. Weakly mineralized Sugarloaf Peak quartz monzonite in road cut. Note oxidation of pyrite in fractures. Basin base levels between the Mesilla and Tularosa/Hueco basin are quite different, with basin elevation in the Tularosa basin near White Sands at 3991 feet and the elevation of Las Cruces at 3896 feet. **(0.3)**

64.5/19.4 Crest of San Agustin Pass. Doña Ana Mountains with Robledo Mountains behind at 10:00 to 11:00. Caballo and Fra Cristobal Mountains at 1:00 and 2:00 respectively. These are all mountain ranges along the eastern edge (Caballos, Fra Cristobals) or within (Robledos, Doña Anas) the Rio Grande rift. View across the Mesilla Valley

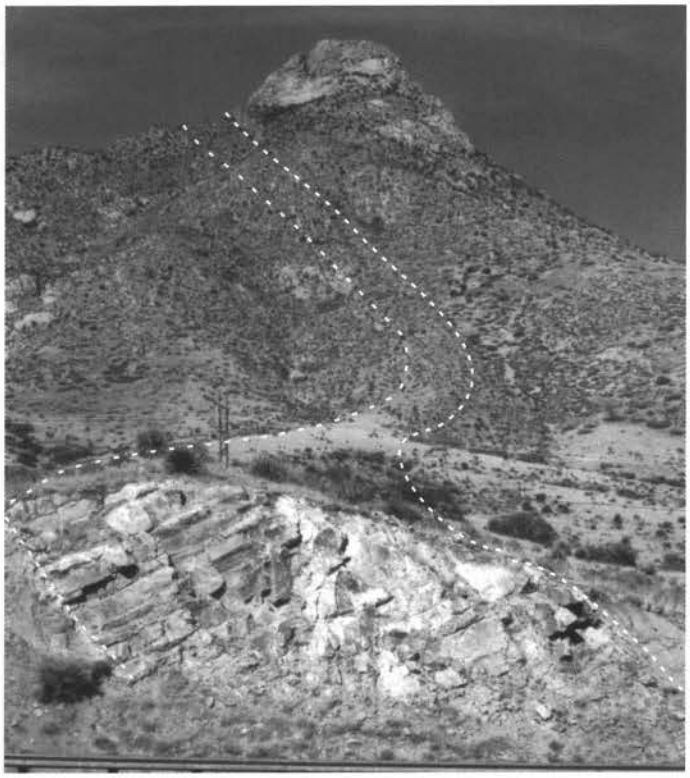

FIGURE 3.14. Felsite dikes trending over San Agustin Peak.

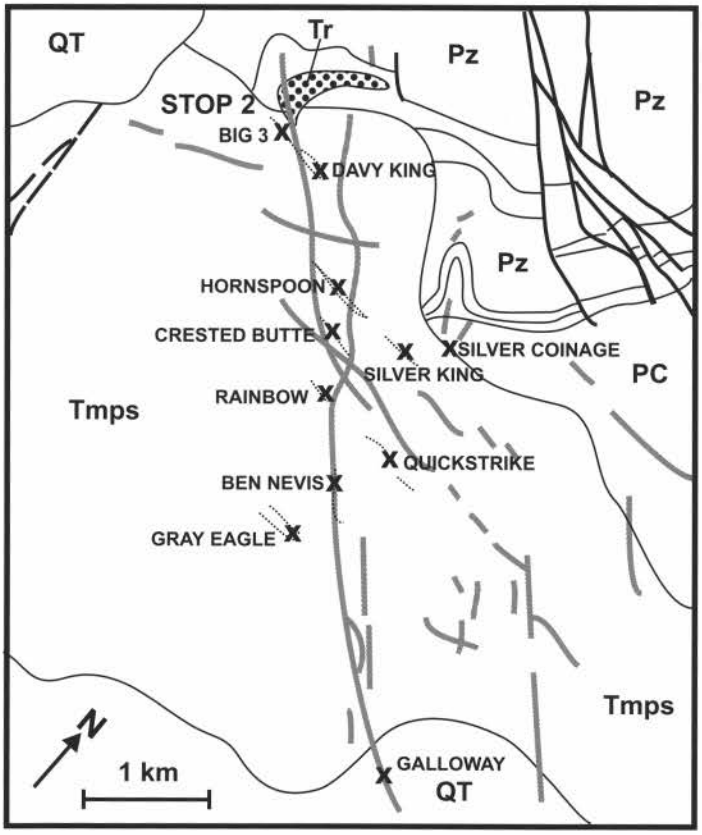

FIGURE 3.15. Map of felsite dikes and associated ore deposits in the San Agustin Peak area (modified from Lueth, 1988). Map units are as follows: QT = Quaternary and Tertiary sediments, Tr = Granite laccolith, Tmps = Sugarloaf Peak Quartz Monzonite, Pz = Paleozoic rocks, Pc = Precambrian rocks. Heavy dark lines are faults. Heavy gray lines are felsite dikes. X = mines. Dotted lines are quartz vein systems.

of the Rio Grande rift. **(1.2)**

65.7/18.2 Historical Marker for the site of San Agustin Springs, where on 27 July 1861, a force of 500 Union soldiers lead by Major Isaac Lynde surrendered to the Confederates. San Agustin Springs on right. **(0.3)**

66.0/17.9 Enter the town of Organ. Torpedo and Copper Bar Mines on left (Fig. 3.16). Organ began in 1881 as a mining camp and reportedly (Julyan, 1996) as many as 1800 people once resided here. By 1890, however, the population was down to about 100, but the town survived, and now is a community of about 500 people, many of whom work at White Sands Missile Range or in Las Cruces.

The Organ district produced substantial amounts of silver, lead, and copper, totaling about $2.5 million (1935 dollars). Approximately half of this value came from the Stevenson-Bennett mine, a few miles to the south, but little mining has occurred since 1935. According to Seager (1981), who summarized the mineral deposits of the Organ district, most of the mineralization is associated with the Sugarloaf Peak quartz monzonite porphyry stock, one of the latest stages of the Organ batholith. The Stephenson ore body was discovered on the surface in the late 1840s and

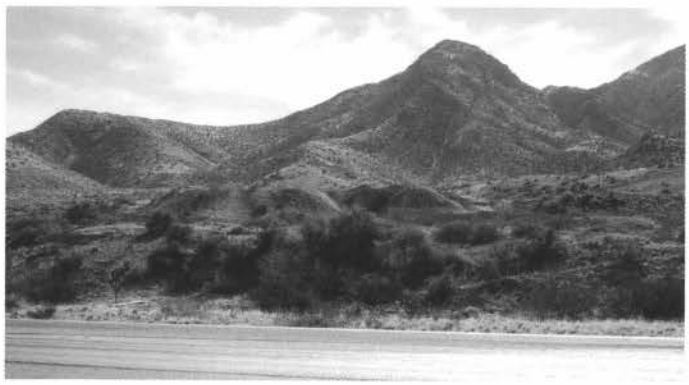

FIGURE 3.16. Torpedo Mine as it appears today.

worked intermittently for silver by crude methods for about 30 years. The coming of the railroad in 1881 and discovery of the Bennett ore body and other deposits in the 1880's stimulated mining, and the district became an important producer of lead as well as silver. Copper production, from veins along faults and replacement bodies in limestone began in 1900, and the greatest combined production of all three metals (about $900,000) occurred from 1900 to 1909 (Dunham, 1935). After a short surge in production during World War I, the Organ district has yielded only small amounts of the three main metals, plus minor amounts of gold and zinc.

The Torpedo mine exploited oxidized copper ores from silicified and brecciated quartz monzonite. The deposit is sandwiched between two faults, with the eastern fault separating the deposit from barren intrusive and the western fault from Pennsylvanian Madera Group rocks (Dunham, 1935). Some of the workings attained a depth of over 600 feet. The low grade primary ore consists of pyrite, chalcopyrite, and quartz, typical of copper breccia pipe deposits (Lueth, 1988). Oxidation of the material resulted in the formation of ore grade deposits of chrysocolla, malachite, azurite, and abundant native copper. Many of these deposits are summarized and characterized in context to the mining district scale metal zoning patterns in Lueth and McLemore (1998). **(0.1)**

66.1/17.8 Turn right on Dona Ana Co. Road D-87. Building is the former "Star Wars Deli" that began business during the Star Wars defense program. **(0.4)**

66.5/17.4 Remains of the Memphis Mine on right (Fig. 3.17). Dunham (1935) states that more work has been done on this property than any other except the Stephenson-Bennett Mine, discussed later. A small smelter was erected on the property in the mid-1880. The deposits are classified as skarn type with massive replacement of Madera Group limestones by calc-silicate minerals, mainly andradite garnet. Both copper and zinc with lesser amounts of lead were produced from this deposit, mainly as chalcopyrite, sphalerite and galena. Some parts of the mine produced copious quantities of the rare tellurium mineral tetradymite. Samples of this material can be found in many museums today. **(0.2)**

66.7/17.2 Water tank on left. Philadelphia mine on the north slope of hill. Homestake mine at 11:00. The Philadelphia and Homestake mines are both small replacement orebodies in limestone adjacent to sills and dikes. In contrast to the Memphis mine, little calc-silicate development occurred in these deposits. The ore mineral was predominantly "argentiferous galena" and secondary base metal carbonates. Most of the ore deposits on the west side of the Organ-San Andres Mountains are localized along the Torpedo-Bennett Fault Zone (Fig. 3.18) **(0.8)**

67.5/16.4 **Bear right** onto Badger Road, entrance to the Organ Quarry. **(0.4)**

67.9/16.0 **STOP 2** – Pull off on right. Looking north, note the western flank of the southern San Andres Mountains, which exposes a thick, westward-dipping section of upper Paleozoic strata, mostly Pennsylvanian Panther Seep Formation overlain by Lower Permian Hueco Group. At the western base of the mountains there is the old Love Ranch, one of the few places where Cretaceous

FIGURE 3.17. The remains of the Memphis mine.

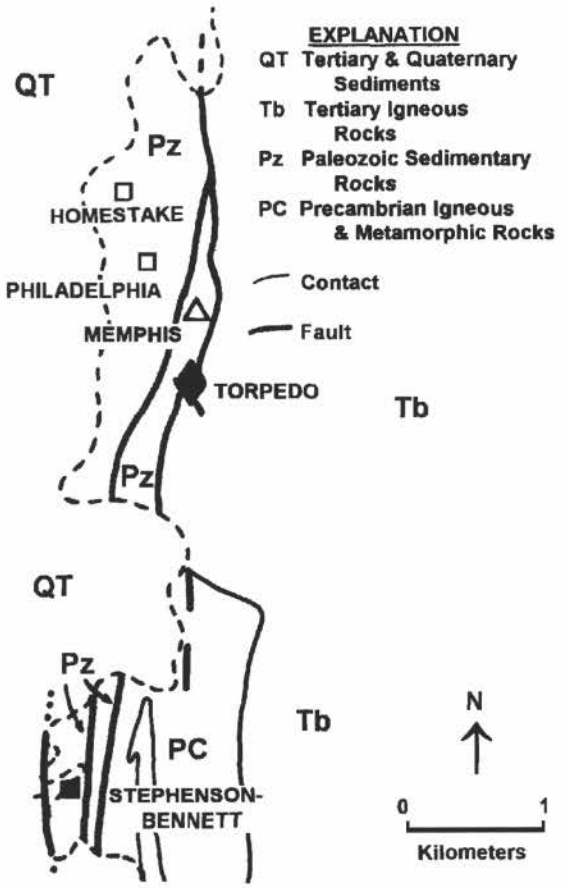

FIGURE 3.18. Generalized geologic map of the Torpedo-Bennett fault zone and associated ore deposits. (modified from Lueth, 1998)

strata (mostly Upper Cretaceous Dakota Sandstone and Mancos Shale) are exposed in the San Andres Mountains (Lucas and Estep, 1998).

At this stop, we will examine the geologic features of the northern margin of the Organ batholith (Fig. 3.19). Most of the features here can be traced to the forceful intrusion of the batholith and associated hydrothermal activity that resulted in a number of ore deposits and extensive metasomatism in the area. The petrologic evolution of the entire Organ cauldron/batholith system has been presented by Seager and McCurry (1988). The overall patterns of ore mineralization in the Organ Mountains have been summarized by Lueth and McLemore (1998). Some of the latest products of batholith crystallization are present as the Excelsior and Galloway flow-laminated felsite dikes and the small, unnamed laccolith that we will examine.

As we walk up the slope toward the top of the laccolith, you will note the country rock consists of Mississippian and Pennsylvanian limestones that have undergone varying degrees of thermal metamorphism and metasomatism. Calc-silicate minerals often are developed on the outer margins of chert clasts. Coarse grained marbles have also been formed from recrystallization of the limestone. Certain beds, typically more argillaceous, may be completely recrytallized to hornfels. Highly permeable horizons are often completely replaced by diopside and occasionally andradite garnets. In places, garnets can be observed as epitaxial overgrowths on pyroxene (diopside) blades.

As we approach the late stage felsite dikes, you will notice increasing alteration and remineralization of the limestones. The felsite dikes are very fine grained and flow laminated. The have been extensively altered and may represent major conduits for late stage hydrothermal fluids, similar to the ore "feeder" dikes at Santa Eulalia, Mexico (Megaw, 1990; Lueth et al., 2000). You might note extensive alteration of the host limestones at the contact with the fine-grained granite laccolith. As you walk into the intrusive body, you will notice extensive, but subtle, dikes and miarolitic cavities. These have been interpreted as fluid exsolution features within the laccolith (Lueth, 1992). On the thickest portion of the laccolith, these dikes and cavities record diffusion-controlled fluid exsolution that resulted in skarn formation on the margins of the intrusive. To the north, dikes and miarolitic cavities disappear, and the laccolith takes on a more fine-grained to glassy character as infiltration processes dominated near a fault. This fault is, in turn, strongly mineralized by quartz, possibly representing

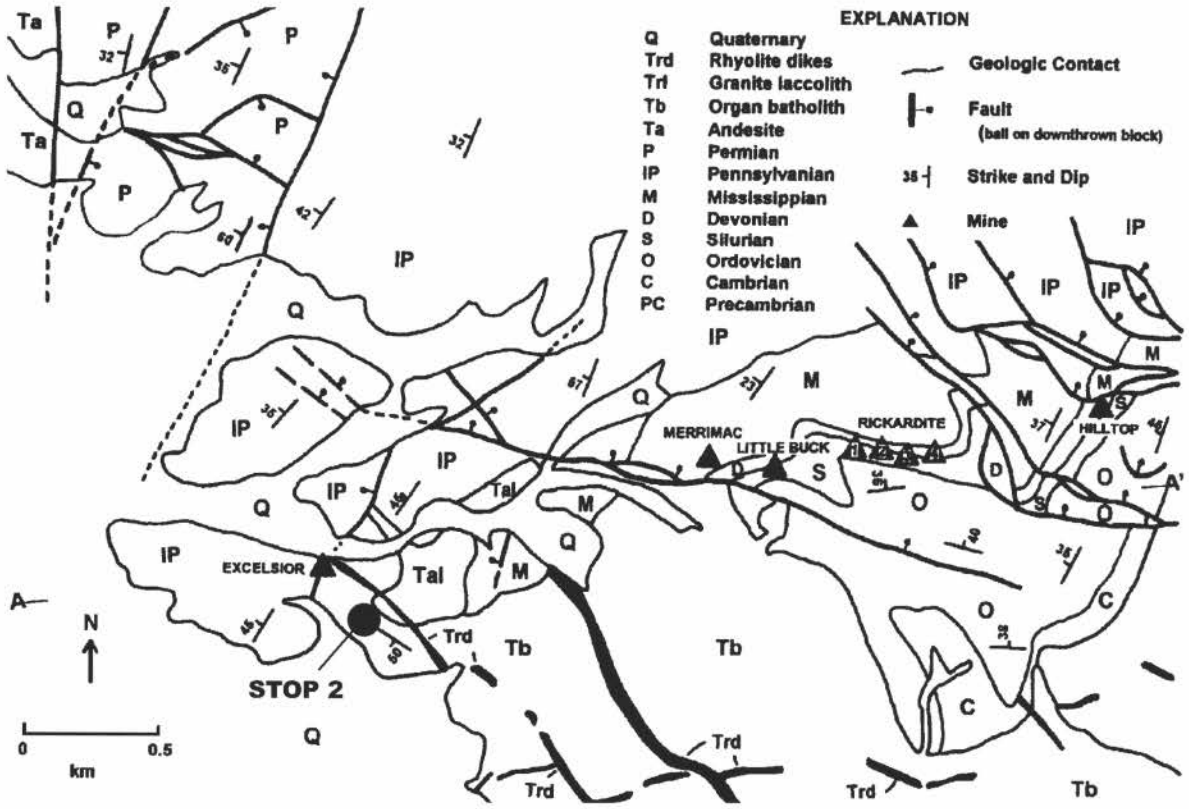

FIGURE 3.19. Generalized geologic map of the northern margin of the Organ Batholith (modified from Lueth, 1998)

the escapeway for exsolved fluids in that portion of the laccolith.

At the top of the hill, the Organ Quarry is in view northeast of the laccolith. The quarry is mining many different rock types on the northern margin of the Organ batholith. A variety of sedimentary rocks each responded differently to the heat and hydrothermal fluids derived from the batholith (Fig. 3.20). The large white areas are massive replacements of limestone by wollastonite. Green rocks are typically skarns or hornfels formed in the more argillaceous units. In this area, the batholith contains abundant pyrite as coating in fractures, similar to that seen at San Augustin Pass. Many small ore deposits are found along the drainage to the east. These deposits are zoned from copper rich skarn at the Excelsior mine, west of the laccolith, to lead-dominated replacement deposits at the crest of the range (Hilltop mine). Lueth and McLemore (1998) attributed this classic zoning pattern to increasing distance away from the Organ copper porphyry deposit (Newcomer and Giordano, 1986) on the pediment west of the laccolith. The deposits east of this laccolith contain tellurium and elevated amounts of precious metals. Lueth (1998) suggested that a second period of mineralization, using the same pathways at those from the porphyry, resulted in an overprinted telluride mineralization event that may have been derived from this late stage intrusive complex.

On the south side of the laccolith, small skarn deposits with weak copper mineralization are present. At the base of the hill, the Big Three vein deposit can be seen. Be careful around the mine openings.

After stop, retrace route back to US-70 in Organ. **(1.8)**

69.7/14.2 Intersection with US-70; **turn right** (west). **(0.2)**

69.9/14.0 Former assay lab of Bentley on right. Note the Florida Mountains in distance at 12:00

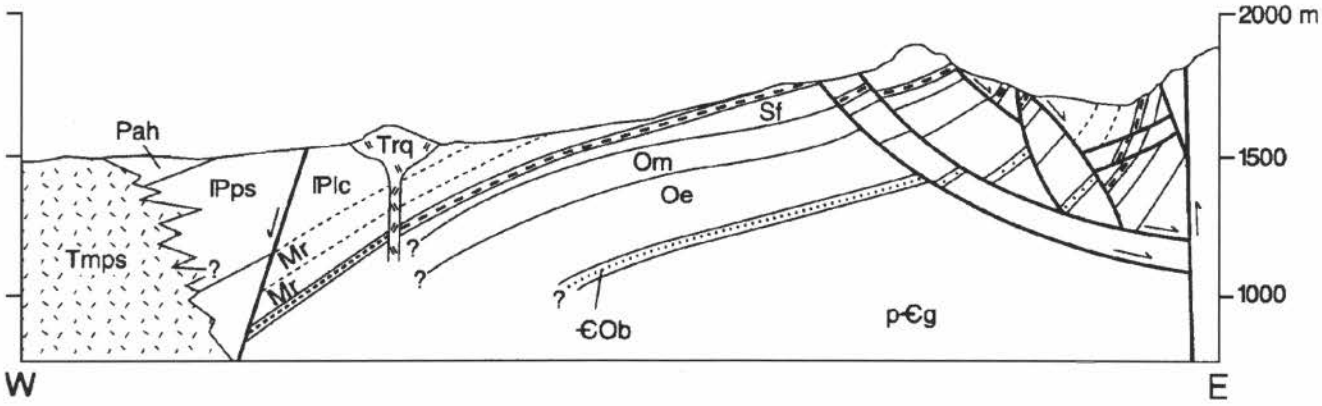

FIGURE 3.20. Geologic cross-section near Stop 2.

and Potrillo Mountains at 10:00. **Merge into left lane. (0.8)**

70.7/13.2 Entrance to NASA Facility on right. **(0.3)**

71.0/12.9 **Turn left,** south, on Baylor Canyon Road. (0.3) Stephenson-Bennett Mine at 10:00. Tortugas Mountain, our final destination, at 1:30. Mount Cox and Riley in the Potrillo Mountains at 2:00 in the distance.

The Stephenson-Bennett mine (Fig. 3.21) represents the most successful mining operation in the Organ Mountains. Discovered in 1847 (Dunham, 1935), early mining was done by mostly primitive methods from the Stephenson orebody – the highest workings on the face of the mountain. The ores were smelted for silver in an adobe furnace down by the Rio Grande. The larger Bennett orebody was discovered in 1882 while driving a tunnel to an extension of the Stephenson orebody at depth (Fig. 3.22), an extension that did not exist. The exploitation of the Bennett orebody resulted in the most profitable period in the mine's history. The smaller Page orebody, between the Stephenson and Bennett orebodies, actually crops out south of the main workings and was developed by small stopes. The orebodies are localized within a fault block transected by a number of post-mineralization faults. They are tabular to elongated replacement deposits consisting of galena, sphalerite, and pyrite in a gangue of quartz, calcite, and fluorite. Extensive oxidation of the upper portions of the orebodies resulted in the formation of a suite of secondary minerals, most notably wulfenite, cerussite and aragonite. Specimens from this mine can be found in museums around the world. Historic documents in the NMBGMR archives reveal specimen mining was underway in the 1880s, making this one of the first operations of its type in the west. **(0.9)**

71.9/12.0 Junction with Sallee Road, continue straight. West face of the range dominated by Organ Needle quartz-monzonite phase of the Organ Batholith. Spires known as the Needles rise to your left. **(0.5)**

72.4/11.5 Cross cattleguard **(0.1)**

72.5/11.4 End of pavement – enter BLM land **(0.4)**

72.9/11.0 Trailhead (small parking lot) for Baylor Canyon Trail on left. **(0.2)**

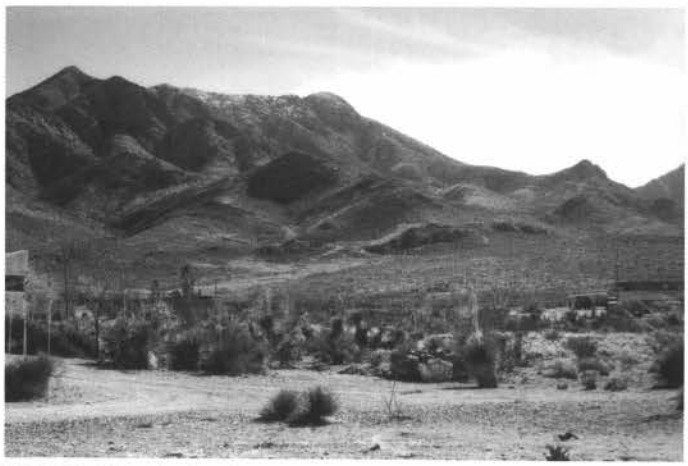

FIGURE 3.21. The Stephenson-Bennett Mine as it appears today.

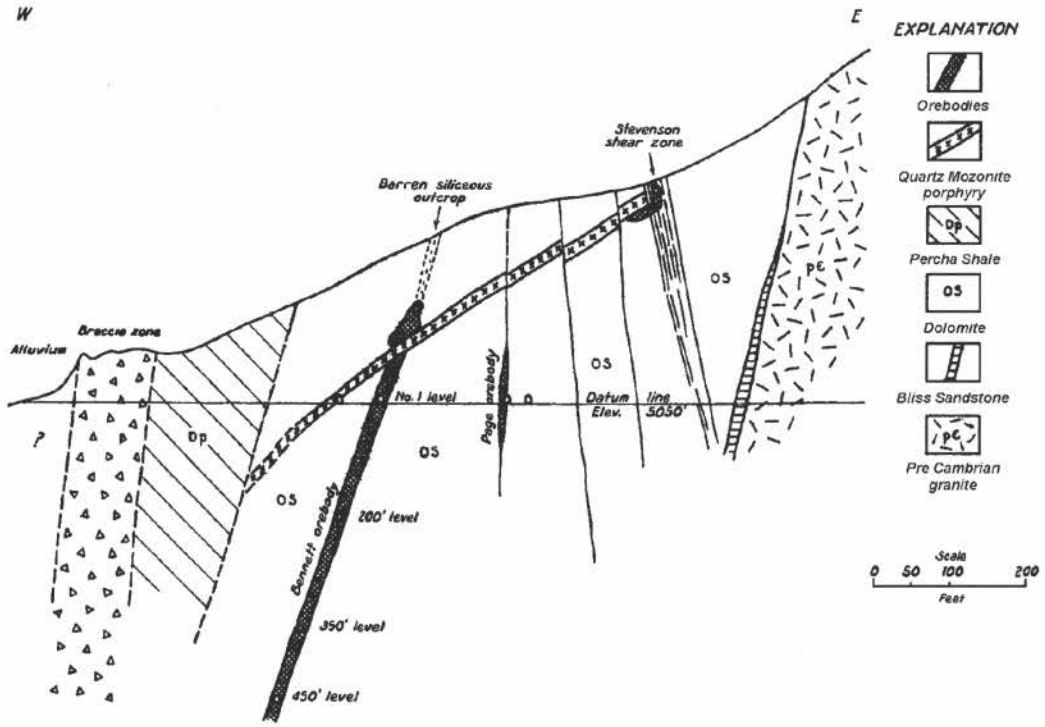

FIGURE 3.22. Cross-section of the Stephenson-Bennett mine as presented by Dunham (1935).

73.1/10.8 Cattleguard **(0.3)**

73.4/10.5 Baylor Peak Road to left. Another small development on an enclave of private land in the BLM tract. **(0.2)**

73.6/10.3 Cattleguard **(1.1)**

74.7/9.2 Cross cattleguard. Road to left to Ruby-Hayner fluorite mine. The mine is located at the top of a talus fan under the "Organ Needles." The fluorite occurs as veins and replacements in metamorphosed and deformed Paleozoic age limestones and shales. The fluorite occurs as tabular lenses. The ore consists primarily of fluorite with significant amounts of calcite, quartz and host rock. Very little barite is present at this property. **(1.0)**

75.7/8.2 Cattleguard. Road to left to Modoc mine. The mine is situated along the Modoc fault zone with a hanging wall of Orejon andesite and footwall composed of Hueco Limestone. The Modoc mine is an irregular skarn and replacement type deposit formed in the Hueco Limestone. Ore minerals consist of chalcopyrite, sphalerite, and galena in a gangue of specular hematite, andradite, epidote, chlorite, quartz and calcite. The Modoc ore body may have been discovered prior to 1854, but production, estimated at $200,000 of lead and silver, occurred from 1879 to 1905 (Dunham, 1935) **(1.0)**

76.7/7.2 Windmill on right. Tortugas Mountain at 2:00 **(0.9)**

77.6/6.3 Stop sign and cattleguard; leave BLM land. Dripping Springs road to left (Fig. 3.23), turn right and head toward Tortugas Mountain. **(1.2)**

FIGURE 3.23. Entrance to the Dripping Springs Recreation area. La Cueva to the lower right.

77.8/6.1 Corral on right. Note Tortugas Mountain and the city of Las Cruces ahead. **(2.5)**

80.3/3.6 Pavement begins; at 12:00 note dumps of former fluorite mines on Tortugas Mountain (A-Mountain to you NMSU Aggies). Tortugas Mountain is a fault block of limestone that rises approximately 500 feet above the bolson floor (Fig. 3.24). The entire fault block dips toward the west. The west and northeast sides of the block are fault bounded.

The fluorite deposits consist of fracture filling of fluorite with minor amounts of calcite and fault gouge. Barite is conspicuously absent. The Tortugas and Jones veins were the primary producers in the district. Some of the ore was acid grade, >99.5 CaF_2 (Johnston, 1928). The majority of the ore was ceramic grade. (Rothrock et al., 1946). **(0.9)**

81.2/2.7 Pass under powerline; note outcrops of Plio-Pleistocene Camp Rice Formation of the Santa Fe Group in creek banks to right. **(0.5)**

81.7/2.2 Cross cattleguard **(1.2)**

82.9/1.0 **STOP 3**, pull off on unpaved road to left. Paleo hot spring deposits of travertine and manganese oxides (Fig. 3.25).

Tortugas Mountain represents the top of a larger horst block that exists in the subsurface (King and Kelley, 1980). The exposed rocks are all mapped as Permian Hueco Formation by Seager et al (1987). The mountain is bounded by faults on all sides that are buried in the subsurface. The entire block is tilted to the west and the southwestern portion of the mountain represents a dip slope. Numerous small faults, trending 0 or 330,° cut through the block (Fig. 3.26). Many of these faults have been mineralized. Extensive silicification and dolomitization is associated with the fault zones in addition to the larger fluorite-calcite deposits mentioned earlier. King and Kelly (1980) estimate the age of mineralization as Miocene.

FIGURE 3.24. Tortugas ("A") Mountain. Can you see the tortuga and which end are you looking at?

FIGURE 3.25. Paleo hot springs at Stop 3.

A small exposure of travertine-manganese oxide mineralization is present in some of the piedmont-slope deposits on the northern end of the mountain. These deposits have been inferred to be of hot spring origin. The rocks in this area have been highly altered and the age of mineralization is estimated to have been during early Camp Rice time (King and Kelly, 1980). The proximity of the Las Cruces Geothermal Field, immediately east of the mountain, to these deposits suggests similar types of mineralization may be occurring in the subsurface today. Accordingly, these travertine-manganese deposits, and the fluorite mineralization as well, may be younger than previously estimated.

Note the extensive gravel pits just north of us developed in fluvial strata of

the Camp Rice Formation (Fig. 3.26). Fossils of proboscideans (elephants and their allies) found in a gravel pit here and just to the north belong to the genera *Stegomastodon*, *Cuvieronius* and *Mammuthus*. This is a rare co-occurrence of these three genera that indicates an early Irvingtonian (early Pleistocene, about 1.5 Ma) age (Lucas et al., 2000). After stop turn left and continue on paved road. **(0.8)**

83.7/0.2 Note cross-bedded sands and gravels of the Camp Rice Formation in the gravel pit to the right. **(0.2)**

83.9/0 Farm and Ranch Museum (Fig. 3.27), turn right to stop for lunch and end of day 3. **(1.1)**

End of Third-day Road Log.

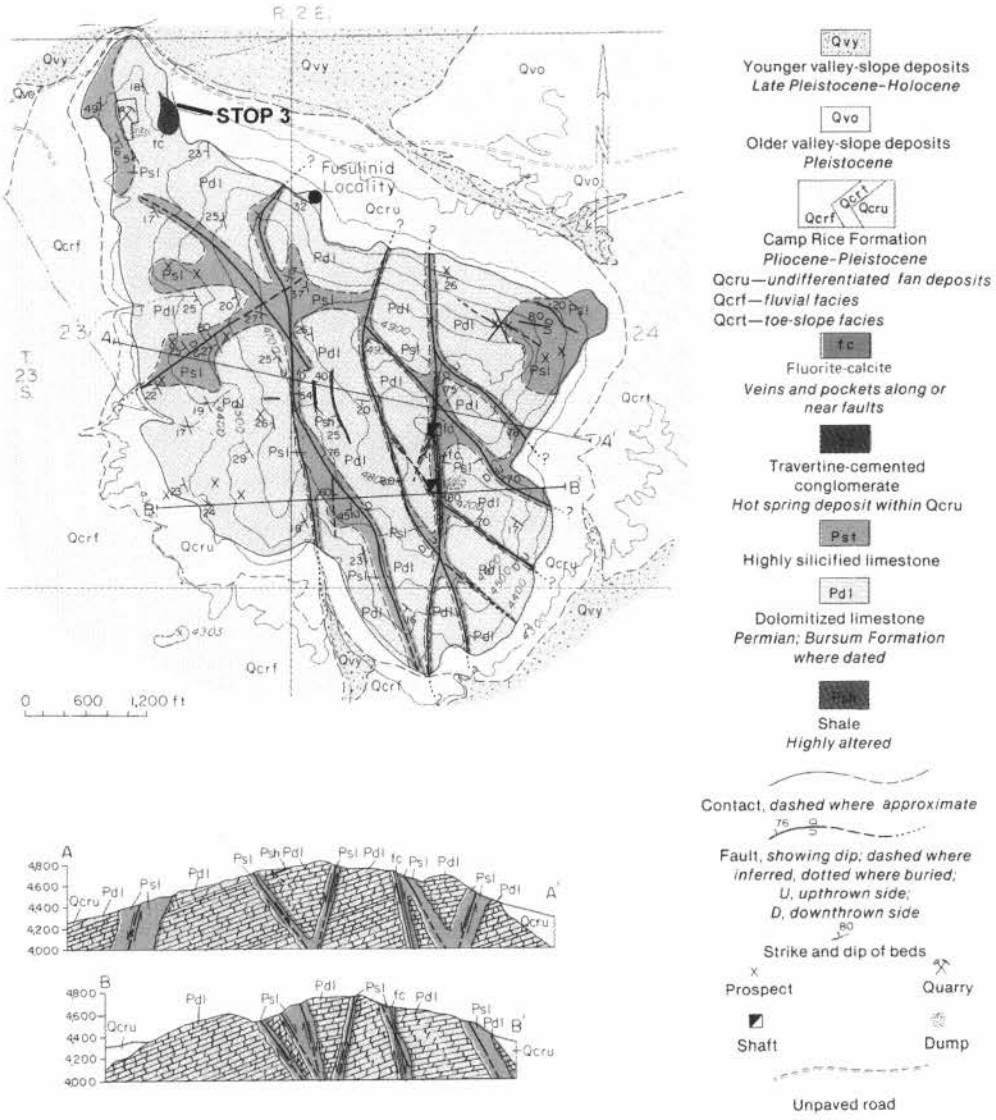

FIGURE 3.26. Geologic map and cross sections of Tortugas Mountain, modified from King and Kelley (1980).

FIGURE 3.27. Gravel pits in Camp Rice Formation that have produced fossils of proboscideans (elephants and their ilk).

FIGURE 3.28. New Mexico Farm and Ranch Museum.

This paper was approved for public release by White Sands Missile Range; distribution unlimited. OPSEC review completed on June 25, 2002.